PNAS RESEARCH ARTICLE | IMMUNOLOGY AND INFLAMMATION

# QSOX1 facilitates dormant esophageal cancer stem cells to evade immune elimination via PD-L1 upregulation and CD8 T cell exclusion

Jia-Ru Wei[a,b,c,1], Baifeng Zhang[d,1], Yu Zhang[e,f,1], Wo-Ming Chen[a,b], Xiao-Ping Zhang[a,b], Ting-Ting Zeng[e], Yan Li[e], Ying-Hui Zhu[e,2], Xin-Yuan Guan[d,e,g,2], and Lei Li[a,b,e,2]

Affiliations are included on p. 11.

Edited by Tasuku Honjo, Kyoto Daigaku, Kyoto, Japan; received April 15, 2024; accepted September 12, 2024

**Dormant cancer stem cells (DCSCs) exhibit characteristics of chemotherapy resistance and immune escape, and they are a crucial source of tumor recurrence and metastasis. However, the underlying mechanisms remain unrevealed. We demonstrate that enriched Gzmk$^+$ CD8$^+$ T cells within the niche of esophageal DCSCs restrict the outgrowth of tumor mass. Nonetheless, DCSCs can escape immune elimination by enhancing PD-L1 signaling, thereby maintaining immune equilibrium. Quiescent fibroblast-derived quiescin sulfhydryl oxidase 1 (QSOX1) promotes the expression of PD-L1 and its own expression in DCSCs by elevating the level of reactive oxygen species. Additionally, high QSOX1 in the dormant tumor niche contributes to the exclusion of CD8$^+$ T cells. Conversely, blocking QSOX1 with Ebselen in combination with anti-PD-1 and chemotherapy can effectively eradicate residual DCSCs by reducing PD-L1 expression and promoting CD8$^+$ T cell infiltration. Clinically, high expression of QSOX1 predicts a poor response to anti-PD-1 treatment in patients with esophageal cancer. Thus, our findings reveal a mechanism whereby QSOX1 promotes PD-L1 upregulation and T cell exclusion, facilitating the immune escape of DCSCs, and QSOX1 inhibition, combined with immunotherapy and chemotherapy, represents a promising therapeutic approach for eliminating DCSCs and preventing recurrence.**

tumor dormancy | esophageal cancer stem cell | T cell exclusion | reactive oxygen species | PD-1/PD-L1

## Significance

Dormant tumors, akin to the Sword of Damocles, can be reactivated after an unpredictable latency period, leading to lethal recurrence. Due to the absence of effective means to eradicate dormant tumors, tumor dormancy represents one of the most formidable challenges in clinical treatment. In this study, we have revealed that quiescent fibroblast-derived quiescin sulfhydryl oxidase 1 (QSOX1) shapes an oxidative niche, facilitating dormant cancer stem cells (DCSCs) to evade immune elimination by up-regulating PD-L1 signaling and promoting the exclusion of CD8 T cells. Conversely, inhibiting QSOX1 in combination with anti-PD-1 therapy and chemotherapy can eradicate DCSCs by enhancing CD8 T cell infiltration in mice, which may represent a promising therapeutic approach to prevent relapse in patients with residual disease.

Tumor dormancy can persist in the body for an extended period, manifesting as cells or minute nodules, and can be triggered to emerge at an unpredictable time. These dormant tumor cells exhibit characteristics of drug resistance and immune evasion, posing a significant source of tumor recurrence and metastasis (1, 2). Given the scarcity of effective methods to monitor and eradicate these dormant cells, tumor dormancy stands as one of the most formidable obstacles in clinical therapy. Thus, there is an urgent to decipher the mechanisms underlying tumor dormancy and identify key targets for eliminating dormant tumor cells, which is extremely critical to solve the problem of tumor recurrence.

Increasing evidence indicates that tumor dormancy or outgrowth depends on crosstalk between tumor cells and their microenvironment. For example, estrogen receptor (ER)-positive breast cancer cells exhibit a dormant phenotype in the lungs of young mice, but an aged or fibrotic microenvironment with high platelet-derived growth factor (PDGF)-C signaling promotes metastatic outgrowth (3). Enriched natural killer (NK) cells in mouse livers sustain dormancy of breast cancer cells via interferon-γ (IFNγ) signaling, but liver injury activates hepatic stellate cells, resulting in NK cell quiescence through the secretion of CXCL12 (4). Similarly, lung inflammation-activated neutrophils awake dormant breast cancer cells by inducing the formation of neutrophil extracellular traps (NETs) (5). Although blocking the factors that activate dormant tumors is crucial for preventing tumor relapse, eradicating dormant tumor cells is the ultimate solution to the tumor recurrence problem. For instance, STING agonists can eliminate dormant disseminated lung cancer cells and prevent spontaneous outgrowth in mice (6). Therefore, therapies targeted at eradicating dormant cells hold promise for significantly improving the survival rates of cancer patients.

Dormant cancer stem cells (DCSCs) possess unlimited proliferation potential and are involved in tumor dormancy and recurrence. Our previous research has shown that dormant tumor masses enrich lung DCSCs, and high levels of insulin-like growth factor 1 (IGF-1) in the microenvironment induce lung cancer recurrence by stimulating the symmetric division of DCSCs (7). Furthermore, the exit from dormancy of brain cancer stem

Competing interest statement: L.L. and J.-R.W. are inventors on a pending patent related to this work (patentee: Sun Yat-sen Memorial Hospital, 11 June 2024; Application No.: 202410743238.7). The other authors declare that they have no other competing interests.

This article is a PNAS Direct Submission.



[1]J-R.W., B.Z., and Y.Z. contributed equally to this work.

[2]To whom correspondence may be addressed. Email: zhuyh@sysucc.org.cn, xyguan@hku.hk, or lilei59@mail.sysu.edu.cn.

This article contains supporting information online at https://www.pnas.org/lookup/suppl/doi:10.1073/pnas.2407506121/-/DCSupplemental.

Published October 21, 2024.

cells (CSCs) can be triggered by chemotherapy (8). However, the mechanism underlying how the tumor microenvironment regulates the dormancy of CSCs is still unclarified. Recent studies have revealed that a collagen-rich extracellular matrix niche maintains the dormancy of colon CSCs (9, 10). While immune surveillance is a pivotal factor in tumor dormancy, DCSCs are capable of evading immune elimination. Leukemia stem cells maintain dormancy and escape T-cell receptor–mediated apoptosis by up-regulating PD-1 signaling (11). Breast DCSCs resist T-cell attack by establishing a local hypoxic niche (12). These findings suggest that elucidating the mechanisms of interaction between DCSCs and their niche could facilitate the development of novel strategies for eradicating dormant tumor cells and preventing aggressive disease recurrence.

Here, we demonstrate that esophageal DCSCs maintain immune equilibrium with cytotoxic Gzmk$^+$ CD8$^+$ T cells by up-regulating PD-L1 signaling in the dormant tumor. Intriguingly, quiescent fibroblast-derived quiescin sulfhydryl oxidase 1 (QSOX1) enhances the expression of PD-L1 in DCSCs and disrupts CD8$^+$ T cell infiltration by shaping the oxidative milieu, which further reinforces tumor mass dormancy. Inhibiting the activity of QSOX1 with its inhibitor Ebselen, in combination with anti-PD-1 and chemotherapy, can disrupt the equilibrium homeostasis of dormant tumors and eradicate residual esophageal DCSCs in mice, suggesting a potential therapeutic approach to prevent relapse for patients with residual disease.

## Results

**Enriched T Cells in the Dormant Esophageal Cancer Microenvironment.** To unravel the underlying mechanisms of tumor mass dormancy, we established progressive and dormant tumors by subcutaneous (s.c.) injection of gradiently diluted murine esophageal cancer cells (mEC2 and mEC25) into C57BL/6 mice (7) (Fig. 1*A* and *SI Appendix*, Fig. S1 *A–C*). When $5 \times 10^6$ tumor cells were injected, progressive tumors (tumor diameter > 5 mm) were clearly observed in most mice within 8 wk. However, approximately 70% of allograft tumors remained dormant for an extended period (dormant period > 24 wk, tumor diameter < 5 mm) when the number of injected cells was $1 \times 10^6$, which were defined as dormant tumors (*SI Appendix*, Fig. S1 *A–D*). Analogous to clinically minimal residual disease (MRD), the levels of immune cells (e.g., lymphocytes, monocytes, and granulocytes) in the blood of mice with dormant tumors were comparable to those of normal mice, whereas those of mice with progressive tumors were significantly increased (*SI Appendix*, Fig. S1*E*). Hematoxylin-eosin staining and immunofluorescent (IF) staining revealed that, in contrast to progressive tumors, dormant tumors formed a stable spherical cavity structure comprising surviving tumor cells and stromal capsule cells 12 wk after tumor cells injection (Fig. 1 *B* and *C* and *SI Appendix*, Fig. S2 *A* and *B*). Specifically, the dormant tumor mass was encapsulated by fibroblasts and immune cells (Fig. 1*C* and *SI Appendix*, Fig. S2 *C* and *D*). Additionally, capillaries were present only in the capsule of dormant tumors, not within the tumor cells itself (*SI Appendix*, Fig. S2*E*). Furthermore, dormant tumors were capable of regrowth after cotransplantation under the skin of immunodeficient nude mice with Matrigel (*SI Appendix*, Fig. S2*F*). IF staining showed that the proportion of Ki67-positive tumor cells in recurrent tumors was higher than that in dormant tumors (*SI Appendix*, Fig. S2*G*). These pathological results suggest the pivotal role of the microenvironment in regulating tumor dormancy and recurrence.

Hence, we performed single-cell RNA sequencing on progressive and dormant tumors to interrogate the interactions between surviving tumor cells and the microenvironment (*SI Appendix*, Fig. S3*A*). After preprocessing for data quality and batch effect removal, a total of 37,082 cells (18,285 cells from progressive tumors; 18,797 cells from dormant tumors) underwent cell clustering analysis. Based on canonical markers, the cell clusters were annotated into 10 cell types, including tumor cells, endothelial cells, fibroblasts, dendritic cells, macrophages/monocytes, mast cells, neutrophils, B cells, NK cells, and T cells (Fig. 1*D* and *SI Appendix*, Fig. S3 *B* and *C*). Cell percentage analysis revealed that progressive tumors contained a higher proportion of tumor cells, whereas dormant tumors were significantly enriched in T cells (Fig. 1*E*). The high level of T cells in the capsule of dormant tumors was further confirmed by IF staining (Fig. 1*F*). Gene expression profile analysis demonstrated that T cells in dormant tumors exhibited high expression of effector molecules (e.g., *Gzmk*, *Nkg7*, *Prf1*), cytokines (e.g., *Ifng*, *Tnf*), chemokines (e.g., *Ccl4*, *Ccl5*), transcription factors (e.g., *Hopx*, *Tox*, *Maf*), and inhibitory receptors (e.g., *Pdcd1*, *Ctla4*, *Lag3*) (*SI Appendix*, Fig. S3*D*). These findings suggest that T cell-mediated antitumor effects may play a pivotal role in maintaining tumor dormancy.

**Gzmk$^+$ CD8$^+$ T Cells Restrict the Outgrowth of Tumor Mass.** Next, we investigated the role of T cells in tumor mass dormancy. First, T cells from dormant and progressive tumors were further clustered into 14 subsets based on canonical markers and functional molecules that have been reported in esophageal cancer (13) (*SI Appendix*, Fig. S4*A*). Intriguingly, dormant tumors contained more cytotoxic Gzmk$^+$ CD8$^+$ T cells than progressive tumors, despite these T cells expressing certain levels of inhibitory molecules, such as *Pdcd1* and *Ctla4* (Fig. 1*G* and *SI Appendix*, Fig. S4*B*). IF staining validated the enrichment of CD8$^+$ T cells, particularly Gzmk$^+$ CD8$^+$ T cells, in the capsule of dormant tumors compared to progressive tumors (Fig. 1*H* and *SI Appendix*, Fig. S4*C*).

*Gzmk* encodes a serine protease, Granzyme K, which is involved in lymphocyte cytotoxicity and cancer progression (14, 15). In vitro cell foci formation assay and western blotting showed that treatment with recombinant mouse Granzyme K protein inhibited the growth and survival of esophageal cancer cells in a concentration-dependent manner (Fig. 1*I* and *SI Appendix*, Fig. S4*D*). The inhibitory effect of Granzyme K (0.1 μg/mL, 24 h) on the proliferation of tumor cells and the promotion of apoptosis were also verified by IF staining using antibody against Ki67 and cleaved caspase 3 (Cl-Casp3) (*SI Appendix*, Fig. S4 *E* and *F*). Similarly, the proportion of proliferating tumor cells (Ki67$^+$ pan-CK$^+$) was significantly higher than that of apoptotic cells (Cl-Casp3$^+$ pan-CK$^+$) in progressive tumors, whereas the proportions of both were comparable in dormant tumors (*SI Appendix*, Fig. S4*G*). To further confirm that GZMK$^+$ CD8$^+$ T cells restrict the growth of dormant tumors, we utilized antibodies to deplete CD8$^+$ T cells or neutralize GZMK in an animal model of tumor dormancy. Results showed that CD8$^+$ T cell depletion and GZMK neutralization could induce dormant tumor recurrence (Fig. 1*J*). IF staining also revealed that the ratio of proliferating to apoptotic tumor cells was increased by CD8$^+$ T cell depletion or GZMK neutralization (Fig. 1*K*). These pieces of evidence suggest that Gzmk$^+$ CD8$^+$ T cells restrict the outgrowth of dormant tumor mass and contribute to the dynamic balance between proliferation and apoptosis of tumor cells in dormant tumors.

**DCSCs Evade Immune Elimination by Activating PD-L1 Signaling.** The high proportion of CSCs in dormant tumors has been uncovered by our previous study (7). Next, we reconfirmed this finding using single-cell RNA sequencing data. First, cell cluster analysis showed that tumor cells could be divided into five subgroups with cluster

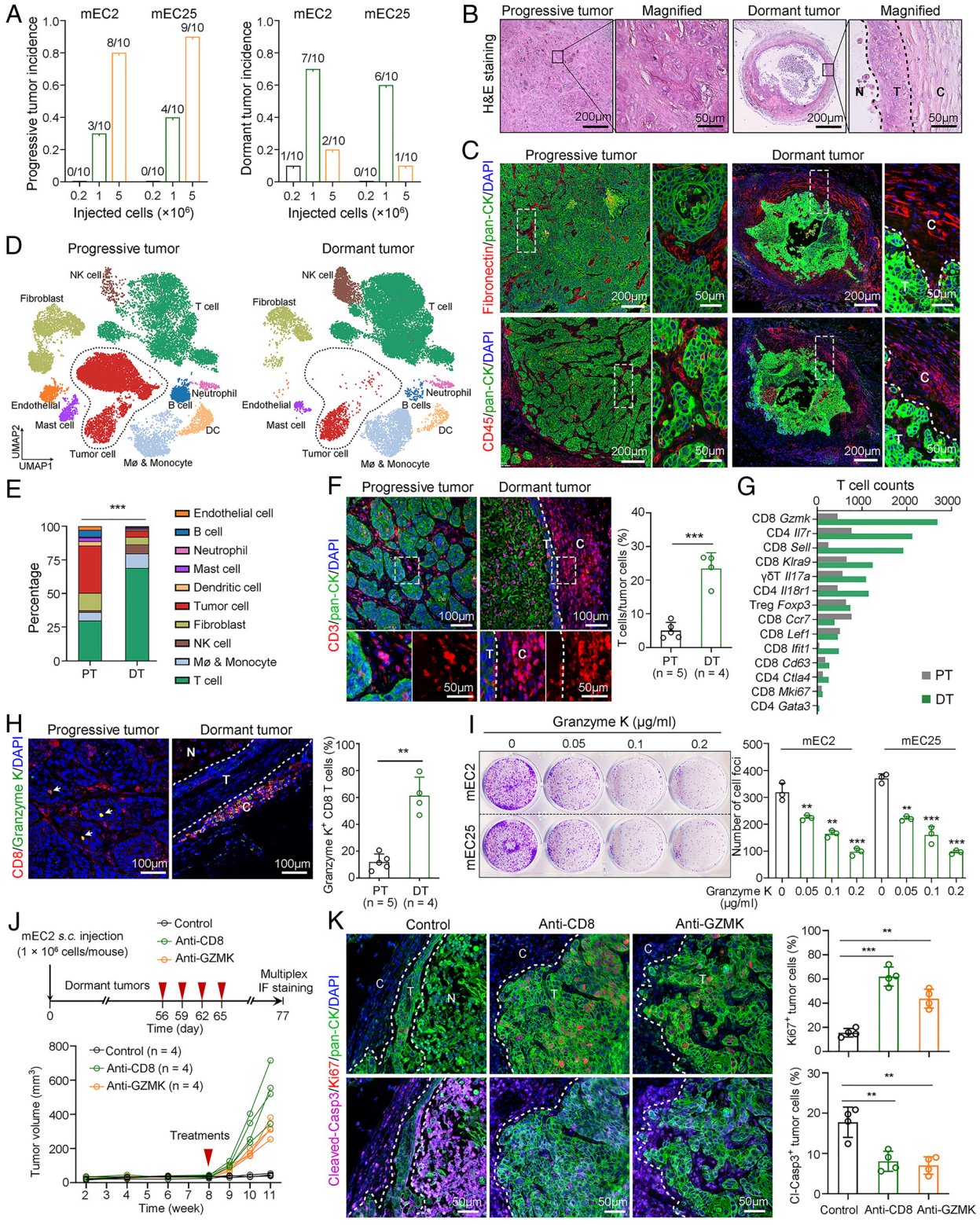


**Fig. 1.** Gzmk$^+$ CD8$^+$ T cells restrict dormant tumor outgrowth. (*A*) The incidence of progressive and dormant tumors in C57BL/6 mice 24 wk after injection of gradiently diluted mEC2 and mEC25 cells ($n$ = 10 mice per group). (*B*) Hematoxylin-Eosin (H&E) staining of progressive and dormant tumors. (*C*) Immunofluorescence (IF) staining of progressive and dormant tumors with antibodies against fibronectin (fibroblasts), CD45 (immune cells), and pancytokeratin (tumor cells). (*D*) 10× Genomics single-cell RNA sequencing was performed to analyze progressive and dormant tumors, and 10 cell types were annotated. (*E*) The percentages of cell types in progressive tumor (PT) and dormant tumor (DT). (*F*) IF staining was used to confirm T cell (CD3$^+$) infiltration in PT ($n$ = 5) and DT ($n$ = 4). (*G*) The counts of T cell clusters in PT and DT. (*H*) The level of Granzyme K$^+$ CD8$^+$ T cells in PT ($n$ = 5) and DT ($n$ = 4) was analyzed using IF staining. (*I*) Foci formation assay of mEC2 and mEC25 cells with treatment of recombinant Granzyme K. (*J*) Antibodies were used to eliminate CD8$^+$ T cells (5 mg/kg, i.v.) or neutralize GZMK (5 mg/kg, i.v.) in an animal model of tumor dormancy ($n$ = 4 per group). (*K*) IF staining showed that the ratio of proliferating to apoptotic tumor cells was increased by CD8$^+$ T cell elimination or GZMK neutralization. In panel (*E*), the $P$-value was calculated using one-way ANOVA, and in panels (*F*), (*H*), (*I*), and (*K*), the unpaired two-tailed Student's $t$-test with Welch's correction was performed for comparisons between two groups. $^{**}P < 0.01$, $^{***}P < 0.001$; ns, no significant difference. All data are presented as mean ± SD. C, Capsule; T, Tumor cell; N, Necrotic core.

C1 being the dominant subgroup in dormant tumors (Fig. 2*A* and *SI Appendix*, Fig. S5*A*). Pseudotime analysis indicated that C1 was at the beginning of the differentiation trajectory, suggesting that this cell subgroup possesses a higher stemness and was defined as CSCs (Fig. 2*B* and *SI Appendix*, Fig. S5*B*). IF staining and western blotting further confirmed the high expressions of esophageal CSC markers (CD44 and CD133) and stemness-associated transcription factors (Oct4A, Sox2, and c-Myc) in dormant tumors compared to progressive tumors (Fig. 2*C* and *SI Appendix*, Fig. S5 *C* and *D*). Additionally, the tumor cells labeled with fluorescent protein GFP were sorted using a fluorescence-activated flow sorter, and sphere formation assay was performed. The results demonstrated that tumor cells derived from dormant tumors exhibited stronger tumor stemness than those derived from progressive tumors (Fig. 2*D*). Consequently, surviving CSCs evade immune elimination and maintain tumor mass dormancy.

Differential gene enrichment analysis showed that tumor cells in dormant tumors were involved in the regulation of T cell activation (Fig. 2*E*). Interestingly, dormant tumors significantly overexpressed the key immune checkpoint *Cd274* (encoding PD-L1) (Fig. 2*F*). Cell communication analysis indicated that PD-1/PD-L1 signaling mediated the interaction between tumor cells and T cells in dormant tumors (Fig. 2*G*). We confirmed higher expression of PD-L1 in dormant tumors compared to progressive tumors by immunohistochemistry (IHC) and double IF staining (Fig. 2*H* and *SI Appendix*, Fig. S6*A*). Importantly, coexpression of CD44 and PD-L1 in esophageal CSCs was found in dormant tumors (*SI Appendix*, Fig. S6*B*). Consistent with the staining results, western blotting also showed higher expression of CD44, PD-1, and PD-L1, as well as Granzyme K and CD8α, in dormant tumors than in progressive tumors (*SI Appendix*, Fig. S6*C*). Furthermore, we confirmed the coexpression of PD-1 and GZMK in $CD8^+$ T cells through multiple IF staining, and found that the proportion of $PD\text{-}1^+$ $GZMK^+$ $CD8^+$ T cells in dormant tumors was higher than in progressive tumors (*SI Appendix*, Fig. S6*D*). We also demonstrated that blocking the PD-1/PD-L1 axis with anti-PD-1 in a tumor dormancy animal model could reduce the volume of dormant tumors by promoting $CD8^+$ T cell infiltration and decreasing the ratio of proliferating to apoptotic tumor cells (Fig. 2 *I*–*K*). In summary, esophageal CSCs evade $PD\text{-}1^+$ $Gzmk^+$ $CD8^+$ T cell-mediated immune elimination by activating PD-1/PD-L1 signaling, resulting in an immune equilibrium state in the dormant tumors (Fig. 2*L*).

**Quiescent Fibroblast-Secreted QSOX1 Promotes PD-L1 Expression.** To explore the molecular mechanism underlying the upregulation of PD-L1 in dormant tumors, we further analyzed the expression levels of differential genes between progressive and dormant tumors. In addition to PD-L1, QSOX1 expression was also markedly up-regulated in dormant tumors (*SI Appendix*, Fig. S7). Critically, *Qsox1* and *Cd274* expressions were positively correlated at the mRNA level in dormant tumors (Fig. 3*A* and *SI Appendix*, Fig. S8*A*). Coexpression of QSOX1 and PD-L1 proteins in dormant tumors was also observed by double IF staining (Fig. 3*B*). Both western blotting and IF staining analyses confirmed that QSOX1 protein expression was higher in dormant tumors than in progressive tumors (*SI Appendix*, Fig. S8 *B* and *C*). Importantly, RT-qPCR and western blotting analyses showed that treatment with recombinant mouse QSOX1 protein (rmQSOX1, 10 ng/mL, 24 h) increased PD-L1 expression in mEC2 and mEC25 cells in a concentration-dependent manner (*SI Appendix*, Fig. S8 *D* and *E*). Vice versa, RT-qPCR analysis revealed that knockdown of *Qsox1* reduced the mRNA expression of *Cd274* in mEC2 and mEC25 cells (*SI Appendix*, Fig. S8*F*). Therefore, high QSOX1 is responsible for the upregulation of PD-L1 in dormant tumors.

QSOX1, as a member of the sulfhydryl oxidase family, has been reported to be expressed in quiescent fibroblasts (16), but why is it highly expressed in dormant tumor? Our cell–cell communications analysis also indicated a strong interaction between fibroblasts and tumor cells in dormant tumors (*SI Appendix*, Fig. S9*A*). Double IF staining showed that the number of activated fibroblasts ($\alpha\text{-}SMA^+$) in dormant tumors was significantly lower than in progressive tumors (*SI Appendix*, Fig. S9*B*). Lower levels of cell division genes (e.g., *Mki67*, *Cdk1*, *Pclaf*) in fibroblasts from dormant tumors compared to those from progressive tumors suggested that quiescent fibroblasts might be involved in the high QSOX1 in dormant tumors (*SI Appendix*, Fig. S9*C*). Next, we confirmed through multiple IF staining that the number of proliferative fibroblasts ($Ki67^+$) in dormant tumors was significantly lower than in progressive tumors (Fig. 3*C*). QSOX1 was highly expressed in both fibroblasts and tumor cells in dormant tumors (Fig. 3D). However, knockdown of *Qsox1* in mEC2 cells did not significantly affect the incidence of dormant tumors (*SI Appendix*, Fig. S9 *D* and *E*). On the contrary, cotransplantation with *Qsox1*-overexpressed fibroblasts significantly promoted the formation of dormant tumors (*SI Appendix*, Fig. S9 *F* and *G*). Intriguingly, both QSOX1 and PD-L1 expression were up-regulated after rmQSOX1 treatment (10 ng/mL, 24 h) of tumor cells, which could be abrogated by treatment with QSOX1 inhibitor Ebselen (10 μM, 24 h) (Fig. 3*E*). These in vivo and in vitro findings suggest that QSOX1 derived from quiescent fibroblasts is responsible for tumor mass dormancy by up-regulating both its own and PD-L1 expressions.

**QSOX1 Shaped Oxidative Niche Up-regulates PD-L1 in DCSCs.** QSOX1 regulates the formation of protein disulfide bond while producing hydrogen peroxide ($H_2O_2$), and $H_2O_2$ serves as a pivotal signaling molecule in modulating reactive oxygen species (ROS) in cancer (17, 18). First, we assayed the concentration of $H_2O_2$ in supernatants derived from homogenized dormant and progressive tumors. The results showed that the level of $H_2O_2$ was elevated in dormant tumors compared to progressive tumors (Fig. 3*F*). Consequently, we analyzed the concentration of $H_2O_2$ in supernatant from mEC2 cells treated with rmQSOX1, with or without Ebselen. Results demonstrated an increased level of $H_2O_2$ after rmQSOX1 treatment, while Ebselen inhibited the activity of QSOX1 to generate $H_2O_2$ (Fig. 3*G*). Additionally, $H_2O_2$ treatment induced the phosphorylation of transcription factor Stat3, aligning with previous studies (19, 20) (Fig. 3*H*). Notably, the protein levels of PD-L1 and QSOX1 were up-regulated in response to increasing $H_2O_2$ concentrations in mEC2 and mEC25 cells (Fig. 3*H*). Bioinformatics analysis revealed a Stat3 binding site on the promoters of *Qsox1* or *Cd274*, respectively (*SI Appendix*, Fig. S10*A*). Chromatin immunoprecipitation-qPCR (ChIP-qPCR) and luciferase reporter assay confirmed that rmQSOX1 treatment up-regulated *Qsox1* and *Cd274* expressions in mEC2 cells via Stat3 activation, and these effects were abolished by Ebselen (Fig. 3*I* and *SI Appendix*, Fig. S10*B*). Furthermore, coexpression of phosphorylated Stat3 with QSOX1 or PD-L1 in allograft tumors derived from mEC2 cells was validated by double IF staining (Fig. 3*J*). Collectively, quiescent fibroblast-secreted QSOX1 shapes the oxidative niche, inducing PD-L1 expression in DCSCs by activating $H_2O_2$/Stat3 signaling.

**Abundant QSOX1 in Dormant Tumor Niche Results in T Cell Exclusion.** It has been reported that increased ROS was associated with a lower level of T cell infiltration in tumors (21). Our above data have shown that T cells predominantly localize in the capsule of dormant tumor and rarely infiltrate the tumor mass (Fig. 1 *F* and *H* and *SI Appendix*, Fig. S4*C*). Therefore, is QSOX1 involved in T cell

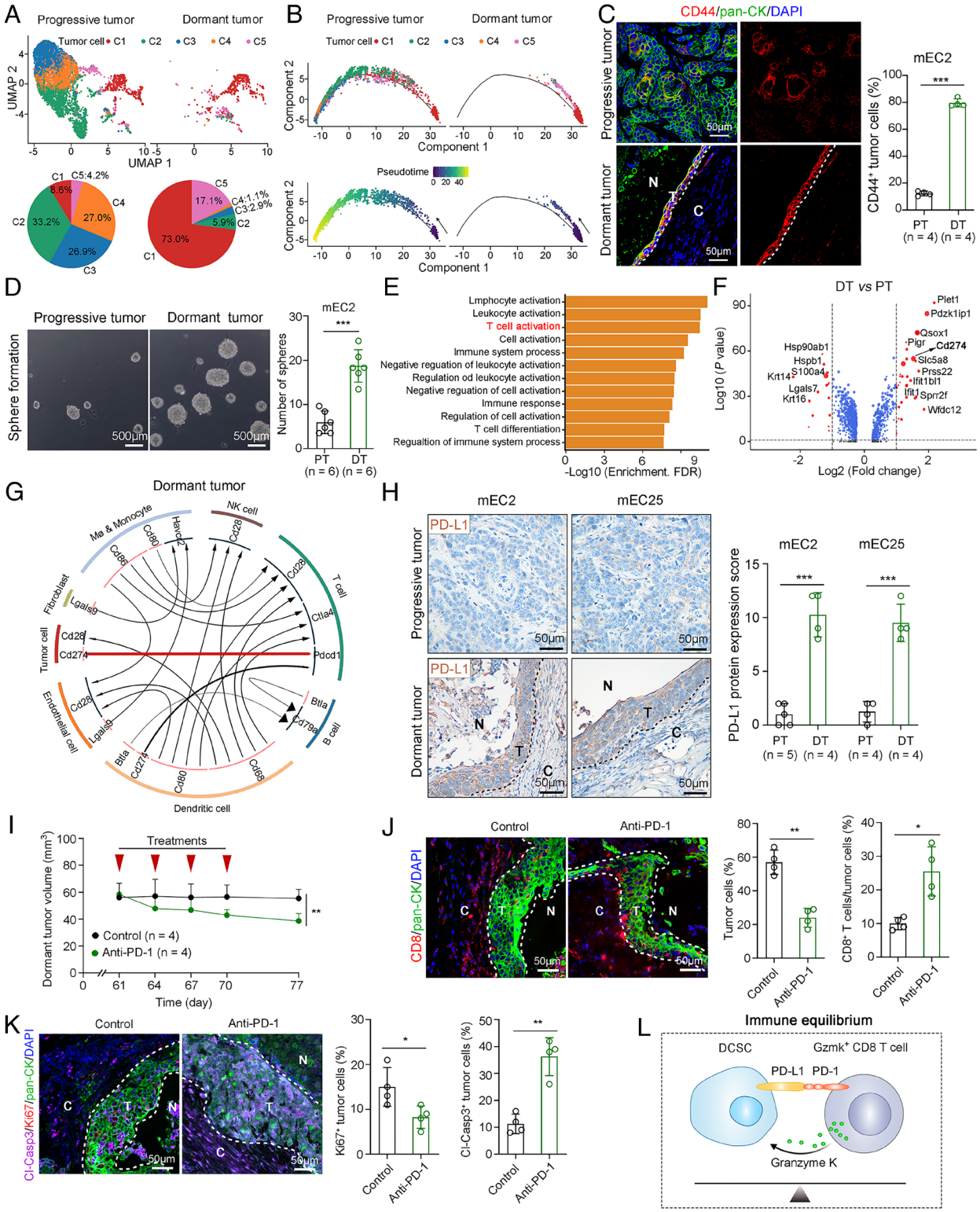


**Fig. 2.** Surviving DCSCs evade immune clearance via upregulation of PD-L1. (*A*) UMAP visualization reveals the subpopulations of tumor cells in PT ($n$ = 5,255 cells) and DT ($n$ = 525 cells) with the percentage of each subpopulation presented in a pie chart. (*B*) Pseudotime analysis of tumor cells using Monocle2. (*C*) IF staining confirms the high level of CD44$^+$ esophageal CSCs in PT ($n$ = 4) and DT ($n$ = 4). (*D*) A sphere formation assay was performed to evaluate the stemness of tumor cells sorted from PT ($n$ = 6) and DT ($n$ = 6). (*E*) Pathway analysis was performed based on the differential genes' expression between tumor cells in dormant and progressive tumors. (*F*) A volcanic plot displays the differential genes in tumor cells between DT and PT. (*G*) Cell communication analysis revealed that PD-1/PD-L1 signaling (encoded by *Pdcd1* and *Cd274*, respectively) mediates the interaction between tumor cells and T cells in dormant tumors. (*H*) IHC staining confirms higher PD-L1 expression in DT compared to PT. (*I*) Dormant tumors were generated by s.c. injection of mEC2 cells ($1 \times 10^6$ cells per mouse). The mice were treated with anti-PD-1 (5 mg/kg, i.v.) 60 d after injection, and the volume of the dormant tumors was measured. (*J*) Double IF staining analyzed the proportion of surviving tumor cells and CD8$^+$ T cells in dormant tumors posttreatment. (*K*) The levels of proliferative (Ki67$^+$) or apoptotic (Cleaved Caspase-3$^+$, Cl-Casp3$^+$) tumor cells were assessed by multiple IF staining. (*L*) Schematic diagram illustrating the immune equilibrium between esophageal DCSC and Gzmk$^+$ CD8$^+$ T cell in dormant tumor. For all panels, *P*-value analyses were performed using the unpaired two-tailed Student's *t* test with Welch's correction. *$P$ < 0.05, **$P$ < 0.01, ***$P$ < 0.001. All data are presented as mean ±SD. C, Capsule; T, Tumor cell; N, Necrotic core.

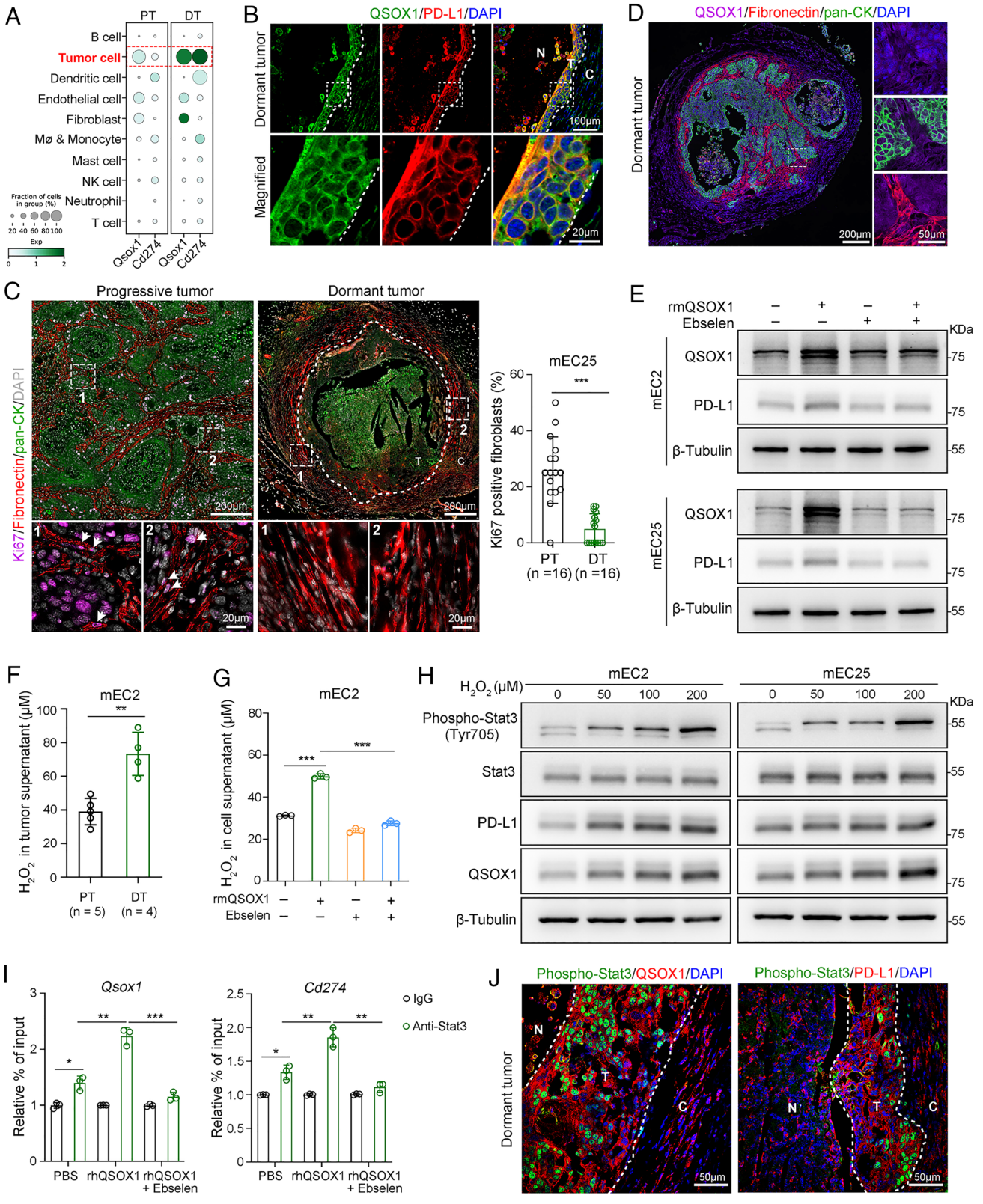


**Fig. 3.** QSOX1 up-regulates PD-L1 by increasing ROS levels in dormant tumors. (*A*) Dot plot shows that both *Qsox1* and *Cd274* (encoding PD-L1) are highly expressed in tumor cells in DT compared to PT. (*B*) Double IF staining showed the coexpression of QSOX1 and PD-L1 in DT. (*C*) Multiple IF staining was used to analyze the level of proliferative fibroblasts (Ki67$^+$ Fibronectin$^+$) in PT and DT. (*D*) Multiple IF staining confirmed that QSOX1 is expressed in both tumor cells and fibroblasts. (*E*) Western blotting revealed that recombinant mouse QSOX1 (rmQSOX1) protein treatment (10 ng/mL, 24 h) up-regulated both itself and PD-L1 in mEC2 and mEC25 cells, while QSOX1 inhibitor Ebselen abrogated this upregulation (10 μM, 24 h). (*F*) After homogenizing dormant and progressive tumors, the concentration of $H_2O_2$ in the supernatants was measured using a commercial kit. (*G*) The level of hydrogen peroxide ($H_2O_2$) in the culture supernatant of mEC2 cells was analyzed 24 h after treatment with rmQSOX1 (10 ng/mL) or/and Ebselen (10 μM). (*H*) The expressions of phosphorylated and total Stat3, PD-L1, and QSOX1 in mEC2 and mEC25 cells were analyzed by western blotting under treatment with $H_2O_2$ at gradient concentrations. (*I*) ChIP-qPCR confirmed that Stat3 transcriptionally regulate the expression of *Qsox1* and *Cd274* in mEC2 cells with treatments with rmQSOX1 (10 ng/mL, 24 h) alone or in combination with Ebselen (10 μM, 24 h). (*J*) Double IF staining confirmed that phosphorylated Stat3 highly coexpressed with QSOX1 or PD-L1 in DT derived from mEC2 cells. In all panels, *P*-value analyses were performed using the unpaired two-tailed Student's *t*-test with Welch's correction. **P* < 0.05, ***P* < 0.01, ****P* < 0.001. Error bars indicate as mean ± SD. C, Capsule; T, Tumor cell; N, Necrotic core.

exclusion? First, multiple IF staining showed that QSOX1 expression was negatively correlated with $CD8^+$ T cell infiltration levels in human esophageal squamous cell carcinoma (ESCC) tissues (Fig. 4*A*). Correlation analysis using The Cancer Genome Atlas (TCGA) data also confirmed this finding across various cancer types, including esophageal carcinoma (ESCA), thymoma (THYM), pancreatic adenocarcinoma (PAAD), skin cutaneous melanoma (SKCM), and others (*SI Appendix*, Fig. S11*A*). In addition, tumors derived from *Qsox1*-transfected mEC2 cells exhibited lower infiltration levels of $CD8^+$ T cells compared to control tumors (Fig. 4*B* and *SI Appendix*, Fig. S11*B*). *Qsox1*-overexpressing mEC2 cells demonstrated a higher propensity for developing tumor dormancy than control cells following the injection of $0.2 \times 10^6$ cells, suggesting a pivotal role for QSOX1 in maintaining tumor dormancy (*SI Appendix*, Fig. S11*C*). Consequently, we performed in vitro chemotaxis assays to investigate the effect of QSOX1 on $CD8^+$ T cell infiltration (Fig. 4*C*). First, $CD8^+$ T cell chemotaxis induced by conditioned media from *Qsox1*-transfected mEC2 and mEC25 cells was weaker than that from vector-transfected tumor cells. Notably, treatment with QSOX1 inhibitor Ebselen (10 μM) restored $CD8^+$ T cells' migration activity under conditioned media from tumor cells with *Qsox1* overexpression (Fig. 4*D*). Moreover, rmQSOX1 supplement inhibited $CD8^+$ T cell chemotaxis induced by tumor cells-derived conditioned media, which could be reversed by treatments with the QSOX1 inhibitor Ebselen (Fig. 4 *E* and *F*) or the antioxidant EUK-134 (*SI Appendix*, Fig. S11 *D* and *E*). Furthermore, when tumor cells were treated with $H_2O_2$, the chemotactic activity of $CD8^+$ T cells induced by conditioned media was also weakened (Fig. 4*G*). Thus, a high level of QSOX1 in the dormant tumor microenvironment reduces $CD8^+$ T cell migration by increasing ROS levels.

Next, we conducted RNA sequencing to elucidate the pivotal genes in $CD8^+$ T cells that are regulated by QSOX1. Primary $CD8^+$ T cells were isolated from mouse peripheral blood and directly exposed to rmQSOX1 (10 ng/mL, 24 h) or PBS (Fig. 4*H* and Dataset S1). Gene ontology (GO) analysis indicated that QSOX1 is involved in lymphocyte migration, cell chemotaxis, and the ROS metabolic process (Fig. 4I). Genes associated with T cell migration, including *Itgb2* (22) and *Cxcr2* (23), were down-regulated following treatment with rmQSOX1, an effect that was reversed by Ebselen treatment (Fig. 4 *J* and *K*). Similarly, the expressions of *Itgb2* and *Cxcr2* in $CD8^+$ T cells were decreased upon supplementation with $H_2O_2$ (100 μM, 24 h) (*SI Appendix*, Fig. S11*F*). Conditioned media from *Qsox1*-overexpressing mEC2 cells also diminished the expressions of *Itgb2* and *Cxcr2* in $CD8^+$ T cells, and this downregulation was rescued by Ebselen (*SI Appendix*, Fig. S11*G*). Thus, elevated QSOX1 levels inhibit T cell migration, further aiding dormant tumors in evading immune eradication, in addition to fostering the expression of PD-L1.

**High QSOX1 Expression Indicates a Poor Response to Anti-PD-1 Treatment.** TCGA analysis revealed that the mRNA expression of QSOX1 in ESCC tissues was lower than that in normal esophageal epithelial tissues (*SI Appendix*, Fig. S12*A*). However, this discrepancy did not affect the overall survival of ESCC patients (*SI Appendix*, Fig. S12*B*). Notably, high QSOX1 expression was associated with a poor prognosis in patients with $CD8^+$ T cell enrichment (*SI Appendix*, Fig. S12*B*). Furthermore, an analysis of reported clinical data on anti-PD-1 treatment in renal cell carcinoma (RCC), lung squamous cell carcinoma (LUSC), and melanoma demonstrated that patients with high QSOX1 expression had a worse prognosis compared to those with low QSOX1 expression (*SI Appendix*, Fig. S12*C*). We also analyzed the correlation between QSOX1protein level and ESCC patient response to anti-PD-1 (Toripalimab) combined with chemotherapy (paclitaxel and cisplatin) treatment. Our findings revealed that ESCC tissues from nonresponders had higher QSOX1 than those from responders (Fig. 5*A*). Consistent with the dormant tumor model observed in mice, IF staining showed that QSOX1 was expressed in both fibroblasts and tumor cells in ESCC tissues from nonresponders (Fig. 5*B*). In contrast to responder, nonresponder had fewer proliferative fibroblasts ($Ki67^+$ $Fibronectin^+$) (Fig. 5*C*). These findings in clinical samples suggest that quiescent fibroblasts may diminish immune response by secreting QSOX1, and thus, targeting both QSOX1 and PD-1 represent an effective strategy for improving patient outcomes.

**QSOX1 Inhibition in Combination with Anti-PD-1 Eliminates Dormant Tumors.** Hence, we evaluated the effect of targeting QSOX1 with Ebselen on tumor dormancy in mouse models. First, dormant tumors were generated by s.c. injection of mEC2 cells ($1 \times 10^6$ per mouse), and mice were subsequently treated with Ebselen (10 mg/kg, i.p.) alone or in combination with anti-PD-1 (5 mg/kg, i.v.) or chemotherapy (paclitaxel, 6 mg/kg, i.p. + cisplatin, 6 mg/kg, i.p.) four times 56 d after the cells were injected. Surprisingly, Ebselen in combination with anti-PD-1 or chemotherapy significantly reduced the volume of dormant tumors, as opposed to Ebselen monotherapy (Fig. 5*D*). IF staining revealed that dormant tumors treated with the combined regimen (Ebselen + anti-PD-1 + chemotherapy) exhibited a higher proportion of apoptotic tumor cells ($Cl\text{-}Casp3^+$) and a lower proportion of proliferative tumor cells ($Ki67^+$) compared to other groups (Fig. 5*E*). Notably, while most $CD8^+$ T cells remained confined to the capsule of untreated dormant tumors, Ebselen, either alone or in combination with anti-PD-1 or chemotherapy, facilitated $CD8^+$ T cell infiltration into the tumor nests (Fig. 5*F*). In summary, inhibiting QSOX1 with Ebselen disrupts the equilibrium of dormant tumors, fosters T cell infiltration, and potentiates the antitumor efficacy of anti-PD-1 and chemotherapy, potentially presenting a highly effective therapeutic strategy for patients harboring dormant tumors (Fig. 6).

## Discussion

QSOX1 is an enzyme that catalyzes disulfide bond formation and $H_2O_2$ production during protein folding (17, 18). We used multiple IF staining to demonstrate that QSOX1 is expressed in both tumor cells and fibroblasts in dormant tumors. Inhibition of QSOX1 secretion from fibroblasts can disturb extracellular matrix remodeling and attenuate tumor growth and metastasis (24). We demonstrated that treatment with recombinant QSOX1 increased the expression of QSOX1 itself in murine esophageal cancer cells, which further elevated the level of $H_2O_2$ in a dormant tumor microenvironment. Consequently, the interactions between CSCs and fibroblasts collectively shape the highly oxidizing microenvironment of dormant tumors. It has been proposed that high ROS up-regulates the expression of PD-L1 in tumor cells by activating Stat3 signaling (25). Our data also showed that $H_2O_2$ treatment increased the phosphorylation level of Stat3 and the protein expression of PD-L1 in tumor cells. Moreover, we confirmed via ChIP-qPCR that Stat3 transcriptionally regulates the levels of both QSOX1 and PD-L1. However, the molecular mechanism by which $H_2O_2$ activates Stat3 signaling has not yet been elucidated. One of possible mechanism is that $H_2O_2$ interacts with its receptor peroxiredoxin-2 (Prx2), thereby transmitting redox regulation to transcription factor (26).

In addition, we also confirmed that abundant QSOX1 reduced the migration and chemotactic ability of $CD8^+$ T cells in vitro, and inhibition of QSOX1 with Ebselen invigorated $CD8^+$ T cell infiltration in mice. These findings suggest an important regulatory

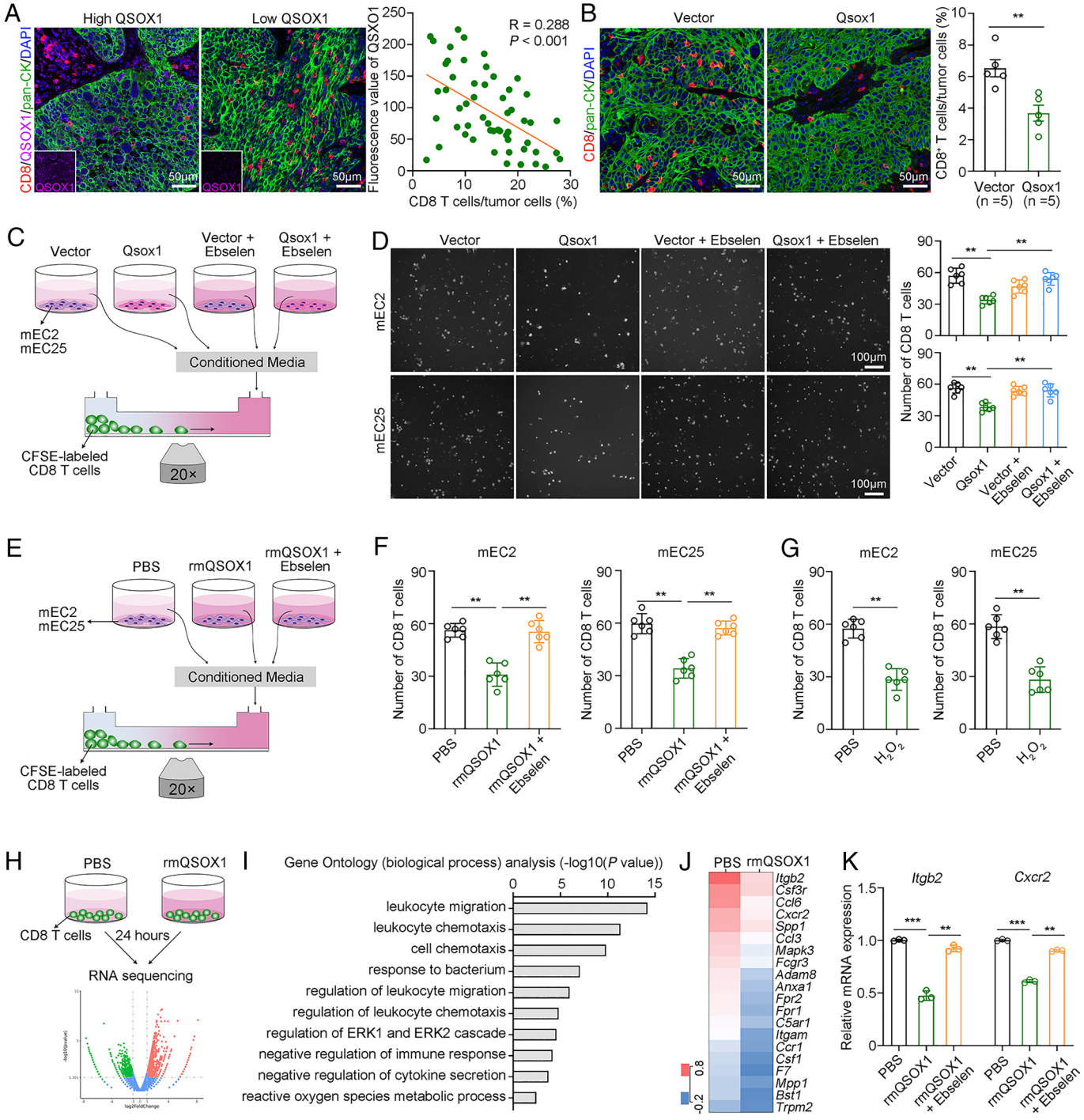


**Fig. 4.** Abundance of QSOX1 inhibits T cell infiltration. (*A*) Multiple IF staining was performed to analyze the correlation between QSOX1 expression and $CD8^+$ T cell infiltration level in ESCC tissues ($n$ = 55 images from 11 samples). (*B*) The infiltration level of $CD8^+$ T cells in tumors derived from *Qsox1*- or vector-transfected mEC2 cells was analyzed by IF staining ($n$ = 5 tumors). (*C* and *D*) Schematic diagram of T cell chemotaxis. *Qsox1*- or vector-transfected mEC2 and mEC25 cells were treated with Ebselen (10 μM, 24 h), and their conditioned media were used for chemotactic T cells in the μ-Slide Chemotaxis (ibidi, #80326). Blood-derived $CD8^+$ T cells were prelabeled with CFSE (5 μM, 10 min). The chemotactic ability of $CD8^+$ T cells was evaluated by counting the number of migrating cells under the microscope. (*E* and *F*) Conditioned media from tumor cells treated with rmQSOX1 alone (10 ng/mL, 24 h) or together with Ebselen (10 μM, 24 h) were for chemotaxis of $CD8^+$ T cells, and the number of migrating $CD8^+$ T cells was counted. (*G*) The effect of $H_2O_2$ on the chemotactic ability of $CD8^+$ T cells was analyzed by adding $H_2O_2$ to the conditioned medium (100 μM, 24 h). (*H*) $CD8^+$ T cells were treated with rmQSOX1 (5 ng/mL, 24 h) or PBS, and RNA sequencing was performed to explore the key genes regulated by QSOX1 in $CD8^+$ T cells. (*I*) GO analysis showed the biological processes regulated by rmQSOX1 treatment. (*J*) Heat map showed the genes that were associated with leukocyte migration and chemotaxis. (*K*) RT-qPCR analysis revealed that T cell migration-related genes *Itgb2* and *Cxcr2* were down-regulated with rmQSOX1, which was rescued by Ebselen. In (*A*), Pearson correlation analysis was used. For other panels, *P*-value analyses were performed using the unpaired two-tailed Student's *t*-test with Welch's correction. $^{**}P < 0.01$, $^{***}P < 0.001$. Data are shown as mean ± SD.

role of QSOX1 in the distribution of T cells, which has not yet been studied. However, a negative correlation between high levels of ROS and T cell infiltration or activation has been reported (21). We revealed that treatments with recombinant QSOX1 or $H_2O_2$ could decrease the expression of T cell migration-associated genes, such as *Itgb2* (22) and *Cxcr2* (23) in T cells. It has been reported that ROS alters DNA methylation pattern during carcinogenesis, which may further inhibit the transcription of *Itgb2* and *Cxcr2* (27, 28). Therefore, inhibiting ROS production can reduce PD-L1 expression and promote T cell infiltration, which may also represent

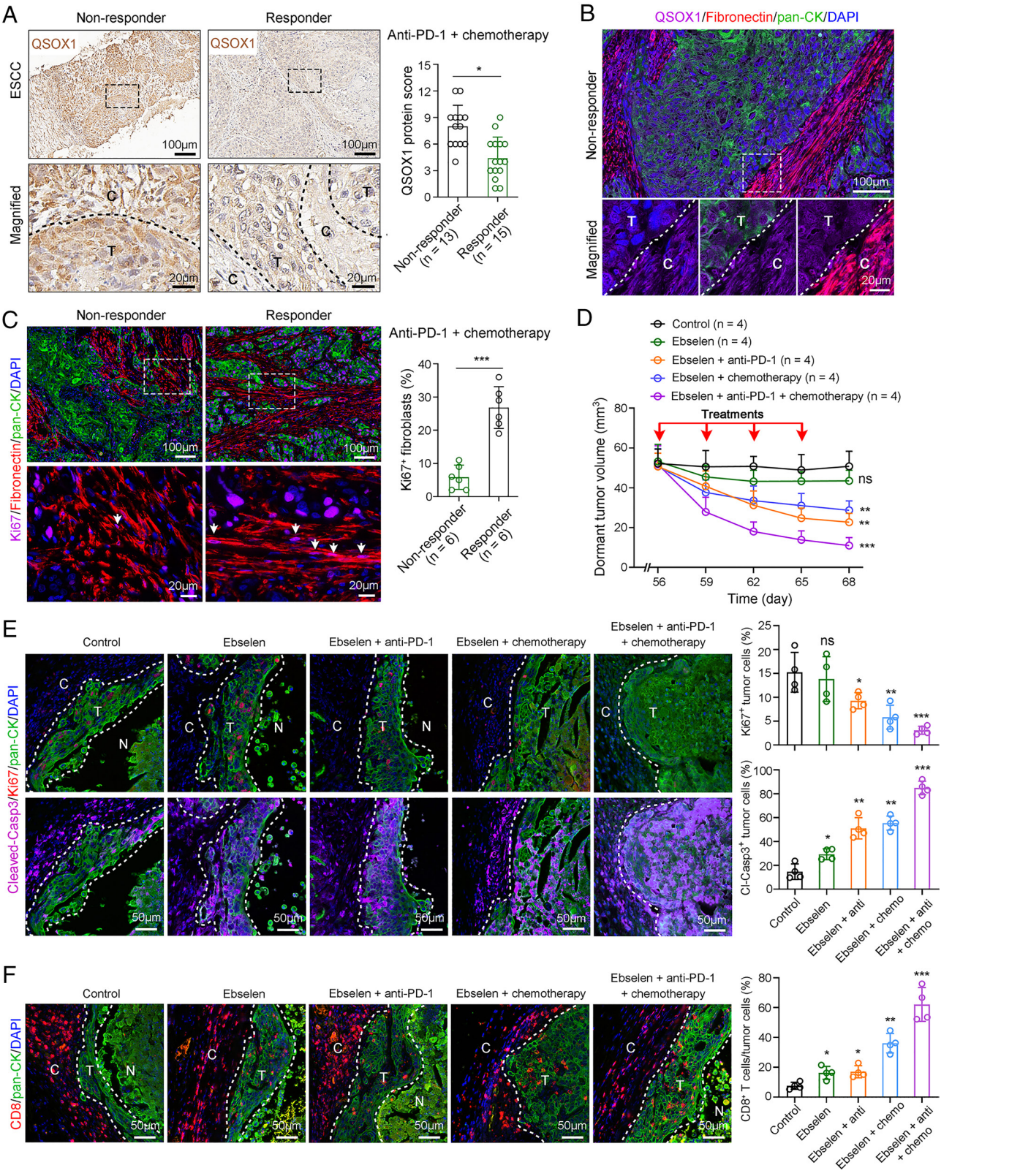


**Fig. 5.** Blocking both QSOX1 and PD-1 in combination with chemotherapy eliminates dormant tumors. (*A*) The protein level of QSOX1 in esophageal squamous cell carcinoma (ESCC) tissues from nonresponders ($n = 13$) or responders ($n = 15$) with anti-PD-1 treatment (Toripalimab) was analyzed by IHC staining. (*B*) Multiple IF staining confirmed the expression of QSOX1 in both fibroblasts and tumor cells in ESCC tissues from nonresponders. (*C*) The level of proliferative fibroblasts (pan-CK$^-$ Fibronectin$^+$ Ki67$^+$) in ESCC tissues from nonresponders ($n = 6$) and responders ($n = 6$) were analyzed by multiple IF staining. (*D*) Dormant tumors were generated by s.c. injection of mEC2 cells ($1 \times 10^6$ cells per mouse). The mice were treated with Ebselen (10 mg/kg, i.p.) alone or in combination with anti-PD-1 (5 mg/kg, i.v.) or chemotherapy (paclitaxel, 6 mg/kg, i.p. + cisplatin, 6 mg/kg, i.p.) four times 56 d after the tumor cells were injected. Carboxymethylcellulose sodium (1% CMC-Na, i.p.) was used as a vehicle for Ebselen. Concurrently with the treatment, the volume of the dormant tumors was measured. (*E*) The levels of proliferative (Ki67$^+$) or apoptotic (Cl-Casp3$^+$) tumor cells were assessed by multiple IF staining. (*F*) Double IF staining analyzed the proportion of CD8$^+$ T cells in dormant tumors posttreatment. For all panels, *P*-values were analyzed using the unpaired two-tailed Student's *t*-test with Welch's correction. $^*P < 0.05$, $^{**}P < 0.01$, $^{***}P < 0.001$; ns, no significant difference. Data are shown as mean ± SD. C, Capsule; T, Tumor cell; N, Necrotic core.

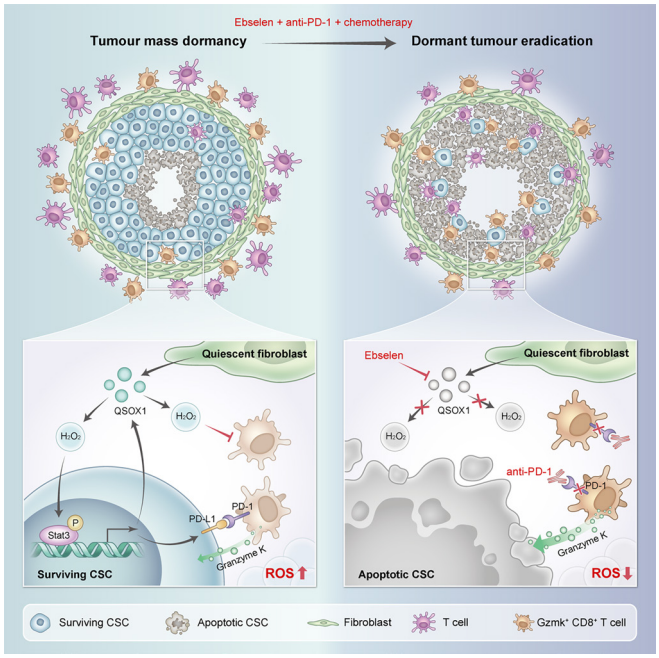


**Fig. 6.** Inhibiting QSOX1 with Ebselen in combination with anti-PD-1 and chemotherapy eradicates residual DCSCs. Quiescent fibroblast-derived QSOX1 shapes the dormant tumor milieu into a highly oxidative state by producing $H_2O_2$, which up-regulates the expression of PD-L1 and itself in DCSCs and facilitates T cell exclusion, resulting in immune equilibrium between DCSCs and PD-$1^+$ Gzmk$^+$ $CD8^+$ T cells. Inhibiting QSOX1 with Ebselen, in combination with anti-PD-1 and chemotherapy, enhances anti-tumor activity and promotes the infiltration of PD-$1^+$ Gzmk$^+$ $CD8^+$ T cells, thereby eradicating residual DCSCs in dormant tumors and preventing relapse.

an important target for eliminating dormant tumors. Immune surveillance has been considered to determine tumor mass dormancy or outgrowth. Our single-cell RNA sequencing data and IF staining results also demonstrated the enrichment of Gzmk$^+$ PD-$1^+$ $CD8^+$ T cells in the dormant tumor niche. The oxidative niche shaped by QSOX1 can promote the expression of PD-L1 by DCSCs and disrupt T cell infiltration into the tumor nest, revealing a mechanism for DCSCs to maintain immune equilibrium with $CD8^+$ T cells. In addition, our finding of endogenous expression of PD-1/PD-L1 in DCSCs to evade immunity further supports the T cell mimicry theory of CSCs (29). For instance, melanoma stem cells express the costimulatory molecules PD-1 and B7-2 (also known as CD86) to preferentially inhibit T cell activation (30). A recent study also reveals that leukemia stem cells express PD-1 to maintain quiescence and protect against T cell receptor-signal-induced apoptosis (11). Moreover, tumor-intrinsic PD-1/PD-L1 inhibits cell proliferation and prevents the interaction with PD-$1^+$ T cells (31). Therefore, a combination therapeutic approach including PD-1 blockade is expected to eliminate DCSCs.

Although treatment with PD-1 blockade combined with chemotherapy has been widely employed as a first-line therapy for esophageal cancer or postoperatively to prevent recurrence, its therapeutic efficacy on residual tumor mass remains uncertain. Our team's previous research results indicated that fibroblasts can activate TGF-β1/Laminin-γ2 pathway in tumor cells, which inhibits T cell infiltration and reduces the efficacy of anti-PD-1, suggesting that it may be challenging to eradicate dormant tumors using anti-PD-1 monotherapy (32). Therefore, we investigated the feasibility of utilizing QSOX1 inhibitor Ebselen in combination with anti-PD-1 and chemotherapeutic drugs to disrupt the immune equilibrium and eliminate dormant tumors in mice. Our results showed that Ebselen combined with or anti-PD-1 or chemotherapy can enhance T cell infiltration and tumor cell apoptosis, whereas the combination can eradicate residual tumor cells. Importantly, we also found that high expression of QSOX1 predicts an adverse response to anti-PD-1 in patients with ESCC. As an anti-inflammatory drug, Ebselen has been used to treat infectious diseases, including SARS-CoV-2 (33) or H1N1 (34) infections. Our findings suggest that Ebselen could also serve as a therapeutic agent to prevent tumor recurrence, particularly for patients with high QSOX1 expression.

In summary, our findings elucidate a mechanism of tumor mass dormancy, whereby the oxidative microenvironment shaped by quiescent fibroblast-derived QSOX1 promotes the immune evasion of esophageal DCSCs through upregulation of PD-L1 signaling and facilitation of T cell exclusion. Inhibition of QSOX1 in combination with anti-PD-1 therapy and chemotherapy enhances $CD8^+$ T cell infiltration and eliminates residual DCSCs in dormant tumors, which may represent a promising treatment strategy for preventing recurrence.

## Materials and Methods

**Mouse Esophageal Cancer Cells and Mice.** The mouse esophageal cancer cell lines mEC2 and mEC25 used in this study were donated by Prof. Li Fu at Shenzhen University (Shenzhen, China) (35). Cell authentication and absence of mycoplasma contamination were confirmed prior to use. Both mEC2 and mEC25 cells were cultured in Dulbecco's Modified Eagle Medium (DMEM, Gibco, #10566016) supplemented with 10% Fetal Bovine Serum (FBS, Gibco, #A5669401) in a 5% $CO_2$ incubator at 37 °C. In this study, male C57BL/6 mice (4 wk old, weight 18 to 20 g) with healthy immune systems were purchased from the Guangdong Medical Laboratory Animal Center (Foshan, China) and housed in the Animal Laboratory Center of Sun Yat-sen University (Guangzhou, China). The mice were maintained in an environment free of specific pathogens. All animal experiments were conducted in strict accordance with the ethical requirements of experimental animal welfare.

**Human Samples.** Cancer tissues from ESCC patients treated with anti-PD-1 therapy (Toripalimab) were collected from Sun Yat-sen University Cancer Center, with all identifying information removed (*SI Appendix*, Table S1). All recruited patients provided written informed consent prior to sample collection, and the study protocol was approved by the Committees for Ethical Review of Research at Sun Yat-sen University (Guangzhou, China). The response to anti-PD-1 drugs was evaluated by Computed Tomography imaging. Patients exhibiting partial response or stable disease were defined as responders, while those with progressive disease were classified as nonresponders.

**Progressive and Dormant Tumor Models.** The mice were preanesthetized and maintained with 1.5% isoflurane. For mEC2 and mEC25 cells, a cell suspension with a gradient cell number ($0.2 \times 10^6$, $1 \times 10^6$, $5 \times 10^6$ cells/mouse) in pure DMEM (100 μL/mouse) was inoculated subcutaneously with a syringe (1 mL) on the right back of the mice. The length and width of the tumor were measured with a vernier caliper, and the tumor volume was calculated as length × width$^2$ × 0.5. According to the ethical and operational norms of experimental animals, the mice were killed by excess $CO_2$ when the tumors were larger than 1 cm in diameter or ulcerated. A tumor with a diameter greater than 5 mm is defined as a progressive tumor. If the tumor diameter remains within 5 mm for a long time (>8 wk), it is defined as a dormant tumor. Progressive and dormant tumors were collected 8 wk after the tumor cells were injected. The tumors were then soaked in Immunol Staining Fix Solution (Beyotime, #P0098) for 24 h, followed by paraffin embedding and staining.

**IF Staining.** The paraffin-embedded tissues were dewaxed with xylene, hydrated with gradient concentration of alcohol, blocked with 5% BSA, and subjected to microwave treatment for antigen retrieval. The primary antibodies (*SI Appendix*, Table S2) were added and incubated at 4 °C for 12 h. Following three times of PBS washing, fluorescently labeled secondary antibodies of different species were applied. After washing with PBS, the tissue sections were mounted with an

antifade solution containing DAPI (Abcam, #ab104139). After 10 min at room temperature, images were captured using a laser confocal microscope (Olympus). The fluorescence intensity of target proteins was analyzed utilizing ImageJ software (https://imagej.net/). Furthermore, multiple IF staining was performed using the Multitarget Immunofluorescence Staining Kit (Panovue, #10001100020) according to the manufacturer's instructions.

**T Cell Chemotaxis Analysis.** The mice were anesthetized and blood was obtained by cardiac blood sampling. Peripheral blood lymphocytes were isolated using Ficoll-Paque PLUS density gradient media (#17-1440-02, GE Healthcare) according to the specifications. $CD8^+$ T cells were sorted by CytoFLEX flow cytometry (Backman) using FITC labeled monoclonal anti-mouse CD8a (eBioscience, #E-AB-F1104C) and labeled with Carboxyfluorescein Succinimidyl Ester (CFSE, 5 μM; GeneCopoeia, #A001) at 37 °C for 10 min. On the other hand, conditioned media from mEC2 or mEC25 cells with different treatments were utilized as chemotactic inducers in vitro. $CD8^+$ T cells and conditioned media were added to the left and right chambers of the μ-Slide Chemotaxis (ibidi, #80326), respectively. Following incubation at 37 °C for 12 h in an incubator containing 5% $CO_2$, the number of migrated T cells was imaged and counted under a fluorescence microscope (Olympus).

**$H_2O_2$ Concentration Detection.** Tumor cells were treated with rmQSOX1 (10 ng/mL) and/or Ebselen (10 μM) for 24 h. The concentration of $H_2O_2$ in the tumor cell culture medium was detected by the Hydrogen Peroxide Assay Kit (Abcam, #ab102500) following the instructions.

**Drug Treatments in Mice With Dormant Tumors.** First, dormant tumors were generated by s.c. injection of mEC2 cells ($1.0 \times 10^6$ cells per mouse). Fifty-six days after cell injection, mice with tumors less than 5 mm in diameter were treated with Ebselen (10 mg/kg, i.p.; TargetMol, #T0825) alone or in combination with anti-PD-1 (5 mg/kg, i.v.; Bio X Cell, #BE0146) or chemotherapy (paclitaxel, 6 mg/kg, i.p.; Selleck, #S1150 + cisplatin, 6 mg/kg, i.p.; Selleck, #S1166) four times every 3 d. Meanwhile, 1% Carboxymethylcellulose Sodium (CMC-Na, i.p.; Sigma, #21902) was used as a vehicle for Ebselen. Tumor volume was measured at the time of administration. Three days after the completion of administration, the mice were weighed and killed with excess $CO_2$. Tumors were collected and immersed in Immunol Staining Fix Solution (Beyotime, #P0098) for 24 h, followed by paraffin embedding and staining.

**Statistical Analysis.** The statistical analysis and graph production for this study were performed using GraphPad Prism 8 software (https://www.graphpad.com/). A two-tailed Student's *t* test with Welch's correction was used to compare difference between two groups. Pearson correlation analysis was used to calculate the correlation between the expression levels of the two genes. The survival probability was estimated using the Kaplan–Meier method, and a univariate Log-Rank test was applied to assess statistical significance by analyzing the *P*-value. If the *P*-value is less than 0.05, the experimental results are considered statistically significant.

**Data, Materials, and Software Availability.** All study data are included in the article and/or supporting information.

**ACKNOWLEDGMENTS.** This work was supported by the National Natural Science Foundation of China (82273474, 82103680, 32471012, 82201231, and 81872007), Guangzhou Science and Technology Project (2023B03J1252 and 2023A03J0715), Guangdong Basic and Applied Basic Research Foundation (2024A1515012989, 2022A1515010068, 2023A1515011593, and 2021A1515010589), Science and Technology Planning Project of Guangdong Province (2023B1212060013 and 2020B1212030004), and Shenzhen Science and Technology Program (ZDSYS20210623091811035 and KQTD20180411185028798). We also thank TosanBio for their help of pattern diagram making.

Author affiliations: [a]Guangdong Provincial Key Laboratory of Malignant Tumor Epigenetics and Gene Regulation, Guangdong-Hong Kong Joint Laboratory for RNA Medicine, Medical Research Center, Sun Yat-sen Memorial Hospital, Sun Yat-sen University, Guangzhou 510120, People's Republic of China; [b]Nanhai Translational Innovation Center of Precision Immunology, Sun Yat-sen Memorial Hospital, Foshan 528200, People's Republic of China; [c]Department of Clinical Laboratory, Sun Yat-sen Memorial Hospital, Sun Yat-sen University, Guangzhou 510120, People's Republic of China; [d]Department of Clinical Oncology, The University of Hong Kong, Hong Kong 00852, People's Republic of China; [e]State Key Laboratory of Oncology in South China and Collaborative Innovation Center for Cancer Medicine, Sun Yat-sen University Cancer Center, Guangzhou 510060, People's Republic of China; [f]Department of Pediatric Oncology, Sun Yat-sen University Cancer Center, Guangzhou 510060, People's Republic of China; and [g]Shenzhen Key Laboratory for Cancer Metastasis and Personalized Therapy, Department of Clinical Oncology, The University of Hong Kong-Shenzhen Hospital, Shenzhen 518000, People's Republic of China

Author contributions: Y.-H.Z., X.-Y.G., and L.L. designed research; J.-R.W., W.-M.C., X.-P.Z., T.-T.Z., and L.L. performed research; J.-R.W., B.Z., Y.Z., and Y.L. analyzed data; and J.-R.W. and L.L. wrote the paper.

1. T. G. Phan, P. I. Croucher, The dormant cancer cell life cycle. *Nat. Rev. Cancer* **20**, 398–411 (2020).
2. S. Gerstberger, Q. Jiang, K. Ganesh, Metastasis. *Cell* **186**, 1564–1579 (2023).
3. F. K. Turrell *et al.*, Age-associated microenvironmental changes highlight the role of PDGF-C in ER(+) breast cancer metastatic relapse. *Nat. Cancer* **4**, 468–484 (2023).
4. A. L. Correia *et al.*, Hepatic stellate cells suppress NK cell-sustained breast cancer dormancy. *Nature* **594**, 566–571 (2021).
5. J. Albrengues *et al.*, Neutrophil extracellular traps produced during inflammation awaken dormant cancer cells in mice. *Science* **361**, eaao4227 (2018).
6. J. Hu *et al.*, STING inhibits the reactivation of dormant metastasis in lung adenocarcinoma. *Nature* **616**, 806–813 (2023).
7. L. Li *et al.*, Expansion of cancer stem cell pool initiates lung cancer recurrence before angiogenesis. *Proc. Natl. Acad. Sci. U.S.A.* **115**, E8948–E8957 (2018).
8. P. Rusu *et al.*, GPD1 specifically marks dormant glioma stem cells with a distinct metabolic profile. *Cell Stem Cell* **25**, 241–257 (2019).
9. Y. Ohta *et al.*, Cell-matrix interface regulates dormancy in human colon cancer stem cells. *Nature* **608**, 784–794 (2022).
10. J. S. Di Martino *et al.*, A tumor-derived type III collagen-rich ECM niche regulates tumor cell dormancy. *Nat. Cancer* **3**, 90–107 (2022).
11. X. Xu *et al.*, PD-1 signalling defines and protects leukaemic stem cells from T cell receptor-induced cell death in T cell acute lymphoblastic leukaemia. *Nat. Cell Biol.* **25**, 170–182 (2023).
12. P. Baldominos *et al.*, Quiescent cancer cells resist T cell attack by forming an immunosuppressive niche. *Cell* **185**, 1694–1708 (2022).
13. X. Zhang *et al.*, Dissecting esophageal squamous-cell carcinoma ecosystem by single-cell transcriptomic analysis. *Nat. Commun.* **12**, 5291 (2021).
14. S. Tiberti *et al.*, GZMK(high) CD8(+) T effector memory cells are associated with CD15(high) neutrophil abundance in non-metastatic colorectal tumors and predict poor clinical outcome. *Nat. Commun.* **13**, 6752 (2022).
15. A. Flemming, GZMK(+) T cells a hallmark of immune ageing. *Nat. Rev. Immunol.* **21**, 1 (2021).
16. D. F. Lake, D. O. Faigel, The emerging role of QSOX1 in cancer. *Antioxid. Redox Signal.* **21**, 485–496 (2014).
17. J. Li *et al.*, QSOX1 regulates trophoblastic apoptosis in preeclampsia through hydrogen peroxide production. *J. Matern. Fetal Neonat. Med.* **32**, 3708–3715 (2019).
18. A. L. Fifield *et al.*, Molecular inhibitor of QSOX1 suppresses tumor growth in vivo. *Mol. Cancer Ther.* **19**, 112–122 (2020).
19. G. Ji *et al.*, Hydrogen peroxide modulates clock gene expression via PRX2-STAT3-REV-ERBalpha/beta pathway. *Free Radic. Biol. Med.* **145**, 312–320 (2019).
20. B. Griess, S. Mir, K. Datta, M. Teoh-Fitzgerald, Scavenging reactive oxygen species selectively inhibits M2 macrophage polarization and their pro-tumorigenic function in part, via Stat3 suppression. *Free Radic. Biol. Med.* **147**, 48–60 (2020).
21. H. Deng *et al.*, Targeted scavenging of extracellular ROS relieves suppressive immunogenic cell death. *Nat. Commun.* **11**, 4951 (2020).
22. L. Wen, M. Moser, K. Ley, Molecular mechanisms of leukocyte beta2 integrin activation. *Blood* **139**, 3480–3492 (2022).
23. Y. M. Khaw *et al.*, Astrocytes lure CXCR2-expressing CD4(+) T cells to gray matter via TAK1-mediated chemokine production in a mouse model of multiple sclerosis. *Proc. Natl. Acad. Sci. U.S.A.* **118**, e2017213118 (2021).
24. T. Feldman *et al.*, Inhibition of fibroblast secreted QSOX1 perturbs extracellular matrix in the tumor microenvironment and decreases tumor growth and metastasis in murine cancer models. *Oncotarget* **11**, 386–398 (2020).
25. X. Zhao *et al.*, High dose Vitamin C inhibits PD-L1 by ROS-pSTAT3 signal pathway and enhances T cell function in TNBC. *Int. Immunopharmacol.* **126**, 111321 (2024).
26. M. C. Sobotta *et al.*, Peroxiredoxin-2 and STAT3 form a redox relay for $H_2O_2$ signaling. *Nat. Chem. Biol.* **11**, 64–70 (2015).
27. Q. Wu, X. Ni, ROS-mediated DNA methylation pattern alterations in carcinogenesis. *Curr. Drug Targets* **16**, 13–19 (2015).
28. Y. Liu *et al.*, DNA methylation of ITGB2 contributes to allopurinol hypersensitivity. *Clin. Immunol.* **248**, 109250 (2023).
29. P. E. Saw, Q. Liu, P. P. Wong, E. Song, Cancer stem cell mimicry for immune evasion and therapeutic resistance. *Cell Stem Cell* **31**, 1101–1112 (2024).
30. T. Schatton *et al.*, Modulation of T-cell activation by malignant melanoma initiating cells. *Cancer Res.* **70**, 697–708 (2010).
31. X. Wang *et al.*, Tumor cell-intrinsic PD-1 receptor is a tumor suppressor and mediates resistance to PD-1 blockade therapy. *Proc. Natl. Acad. Sci. U.S.A.* **117**, 6640–6650 (2020).
32. L. Li *et al.*, Laminin gamma2-mediating T cell exclusion attenuates response to anti-PD-1 therapy. *Sci. Adv.* **7**, eabc8346 (2021).
33. F. Ali *et al.*, Ebselen: A review on its synthesis, derivatives, anticancer efficacy and utility in combating SARS-COV-2. *Mini Rev. Med. Chem.* **24**, 1203–1225 (2024).
34. D. Chen *et al.*, Inhibition of H1N1 influenza virus-induced apoptosis by Ebselen through ROS-mediated ATM/ATR signaling pathways. *Biol. Trace Elem. Res.* **201**, 2811–2822 (2023).
35. T. Huang, J. Yang, B. Liu, L. Fu, A new mouse esophageal cancer cell line (mEC25)-derived preclinical syngeneic tumor model for immunotherapy. *Cancer Commun.* **40**, 316–320 (2020).